Title: **Wind Induced Structure Responses Study on RCCQ Project**

Authors: Xiangdong Du, Technical Director, RWDI
Aaron Wang, Structural Director, CapitaLand Limited
Jon K. Galsworthy, Principal & General Manager, RWDI
Greg Thompson, Senior Project Manager, RWDI

Subjects: Building Case Study
Wind Engineering

Keywords: Climate
Context
Microclimate
Skybridges
Structural Engineering
Supertall
Wind Loads
Wind Tunnel Testing

Publication Date: 2016

Original Publication: Cities to Megacities: Shaping Dense Vertical Urbanism

Paper Type:
1. Book chapter/Part chapter
2. Journal paper
3. **Conference proceeding**
4. Unpublished conference paper
5. Magazine article
6. Unpublished

Wind Induced Structure Responses Study on RCCQ Project

重庆来福士广场项目的复杂结构风致结构响应分析

Xiangdong Du | 杜向东
Technical Director | 技术总监

RWDI | 安邸建筑环境工程咨询有限公司

Guelph, Canada | 圭尔夫，加拿大

Xiangdong Du is the technical director and executive general manager of RWDI China Inc. His areas of specialization at RWDI are cladding and structural wind loads on tall buildings and large roofs. He previously worked in the CFD consulting group.

杜向东博士是RWDI的项目专家，他现在担任RWDI中国分公司（安邸建筑环境工程咨询（上海）有限公司）总监。他在RWDI的专业领域包括高层建筑和大跨场馆屋顶结构的幕墙设计风压和结构风荷载，他工作于计算流体动力学（CFD）组。

Jon Galsworthy
Prinicipal & General Manager
总监、总经理

RWDI | 安邸建筑环境工程咨询有限公司

Guelph, Canada | 圭尔夫，加拿大

Jon Galsworthy is a Principal of RWDI and leads the Loads & Effects Group consisting of more than 100 talented engineers and professionals working together across North America, the UK and Asia.

作为RWDI公司的董事，Jon Galsworthy博士领导着由超过百名优秀的工程师和专家组成的、分布在北美、英国和亚洲的RWDI“风工程–荷载与影响”全球团队。

Greg Thompson
Senior Project Manager | 高级项目经理

RWDI | 安邸建筑环境工程咨询有限公司

Guelph, Canada | 圭尔夫，加拿大

Greg Thompson joined the RWDI Group Companies in 2003 as a Technical Coordinator. As Senior Project Manager, he is responsible for the coordination and supervision of wind load, PLW, snow, air quality, noise/vibration, and CFD studies.

格雷格于2003年作为项目技术人员加入RWDI。作为项目经理，他负责协调和管理风荷载、行人高度风环境、雪、日照/遮阳、空气质量、噪音和振动、计算流体动力学（CFD）的研究。

Aaron Wang | 王隽
Structural Director | 结构设计总监

CapitaLand China
凯德中国(CLC)

Shanghai, China | 上海，中国

Dr. Aaron Wang is a highly competent engineering and project director, chartered civil and structural engineer, builder, and surveyor with nearly 15 years' established international and local professional experience in engineering design and R&D, multi-disciplinary technical, contractural and construction management of commercial and residential building projects.

王隽博士在土木、结构、建设和检验方面是一位能力很强的工程和项目总监，他有近15年的国际和当地的工程设计、技术研发、合同和施工管理的商业和住宅项目经验。

Abstract | 摘要

The Raffles City Chongqing project is one of the largest developments in the world. Located between Chao Tian Men Square and Jiefangbei in Yuzhong District, Chongqing China, it is a curved line of eight towers 182–310 meters tall, bent to resemble masts. A bridge (called conservatory) connecting Towers 2 and 5 passes through towers T3N and T4N and structurally link these 4 towers. In addition to the bridge, wind load challenges include multi-tower interference and the complex local terrain. Due to the complex wind loading, RWDI and CapitaLand conducted tests to the structural model in RWDI's wind tunnels. RWDI obtained site wind profiles incorporating the effect of nearby hills and mountains through topographical study. Both High Frequency Force Balance and Pressure Integration methods were used in the wind-induced structural response study. The wind loads thus obtained were then used for the structural design. A multi-force-balance system was used to analyze.

Keywords: Multi-Structure, Topographical Wind Field Measurement, Wind Induced Structure Responses, Wind Loads

重庆来福士广场项目是世界上最大的发展之一，位于中国重庆渝中区的朝天门广场和解放碑之间，这是项目由182到310米高的8座超高层塔楼组成，形似桅帆。一座连桥（称为景观连廊）将塔楼2，3N、4N和5结构相连。除了结构连桥，风荷载的挑战还包括多塔干扰和复杂的局部地形。由于复杂的风荷载，RWDI和凯德置在RWDI的风洞中进行了结构风响应模型试验。RWDI通过地貌风洞试验研究得到了受山地影响的现场附近的风速剖面。在结构响应研究中，高频天平测力和高频压力积分法均得到应用，由此得到的风荷载用于结构设计。实验使用了多结构天平测力系统。

关键词：多体结构、地貌风场测量、风致结构响应、风荷载

Introduction

Wind induced structural loads on structurally linked towers are extremely complicated and require high-level wind tunnel testing and engineering analysis. The linkages can be in different forms, such as podiums, sky bridges, and others. Two important effects are of the greatest concern to designers: (a) Due to the proximate nature of the towers, wind flows can cause complicated effects between the towers, such as shelter effect and wake buffeting, and (b) different structural responses of individual towers result in the transfer of loads through the structural linkages. Therefore, in order to provide viable design data for responses to the wind, multi-structure testing and analysis must be conducted for linked structures.

The multi-force-balance (MFB) method (Reinhold, 1977; Xie, 2001) considers each tower as being mounted on an individual high-frequency force-balance and tested as an individual substructure. The links between the substructures are disconnected. The tests ensure only the wind loads on each substructure are measured by the

引言

对于结构连体的多塔建筑，风致结构响应分析极为复杂，为此需要更精细的风洞试验和更深入的工程分析。结构连体可以有多种形式，如：裙楼、天桥及其他结构。建筑师最为关心的两个效应为：（a）由于各塔相互接近，气流在塔间可造成复杂的风效应，比如遮挡效应和尾流激振。（b）由于结构连体引起的单塔结构响应。因此，为了提供风致结构响应的设计数据，必须进行连体结构的多结构测试和分析。

多天平测力法（Reinhold，1977，Xie，2001）考虑每一个塔结构为独立自结构并被安置在单一的测力天平上，连体结构相互断开连接，该种测力试验只保证各子结构在同一时间进行测试。高频测压试验（HFPI）（Irwin，1995）在同一时间测量分布在塔和连体上的测压点风压，在分析时，通过积分同一时间内测得的表面风压得到结构响应。对高频测力试验和高频测压试验对单一结构的比较（Dragoiescu C，2006）表明此两种方法结果一致。然而，对于多结构系统，测力法和测压法的比较还没有进行过任何研究。为此，本文进行了多天平测力和高频测压试验的比较。 当建筑设计中包含复杂细节时，如阳台、肋

corresponding force balance simultaneously. The analysis uses the simultaneous loads on each tower to account for their structurally linked nature. The high-frequency-pressure-integration (HFPI) testing (Irwin, 1995) then measures the pressure taps that are distributed on all towers and linkages. During the analysis, the simultaneous pressures are integrated and wind induced multi-structure responses are obtained. The comparison of the high-frequency–force-balance (HFFB) method and the HFPI method are studied for single structures (Dragoiescu C, 2006) and shows good agreement between the two methods. However, multi-structure systems have not been studied. This study presents results and comparison between MFB and HFPI. When the architect designs have complicated features, such as balconies, fins, etc., the constraints of HFPI exist and the tributary areas of taps must be correctly calculated. Hence, in this study, the number of taps and the tap layout are carefully designed with engineering judgement and experience.

The structure design on linked towers must consider: (a) The overall loads on the whole structure, including correlations and phases from each substructures, and (b) the interacting loads between the substructures, including loading transferred through the linkage and the loads on the linkages induced by individual towers (Xie, 2005).

The Raffles City Chongqing (RCCQ) project is one of the largest developments in the world. Located between Chao Tian Men Square and Jiefangbei in Yuzhong District, Chongqing, China, it is a curved line of eight towers 182m to 310m tall, each bent to resemble masts. A conservatory atop Towers 2 and 5 passes through four other towers. From Figure 1, one can see the towers have a complex geometry, such as large numbers of balconies. In order to obtain reliable results, both high-frequency-force-balance (HFFB) and HFPI methods were used in the wind-induced structural response study (Figure 1). The winds loads thus obtained were then used for the structural design. An MFB system was used to analyze the structurally linked towers.

In addition to the linked bridge, wind load challenges included multi-tower interference and the complex local terrain. The site wind profiles incorporating the effect of nearby hills and mountains through topographical wind field measurements were also obtained by wind tunnel measurements.

This paper presents the wind profile simulation method and results from the topographical wind field measurement and analysis. Further, wind induced structural responses are discussed, including wind loads further on the linked intermediate towers.

Experimental Setup

General Setup

The studied building complex consists of eight towers, as shown in Figure 2. The structure plan can be seen in Figure 3. Six towers have connecting linkages in the form of sky bridges. There are walking bridges connecting Towers 3N and 3S and Towers 4N

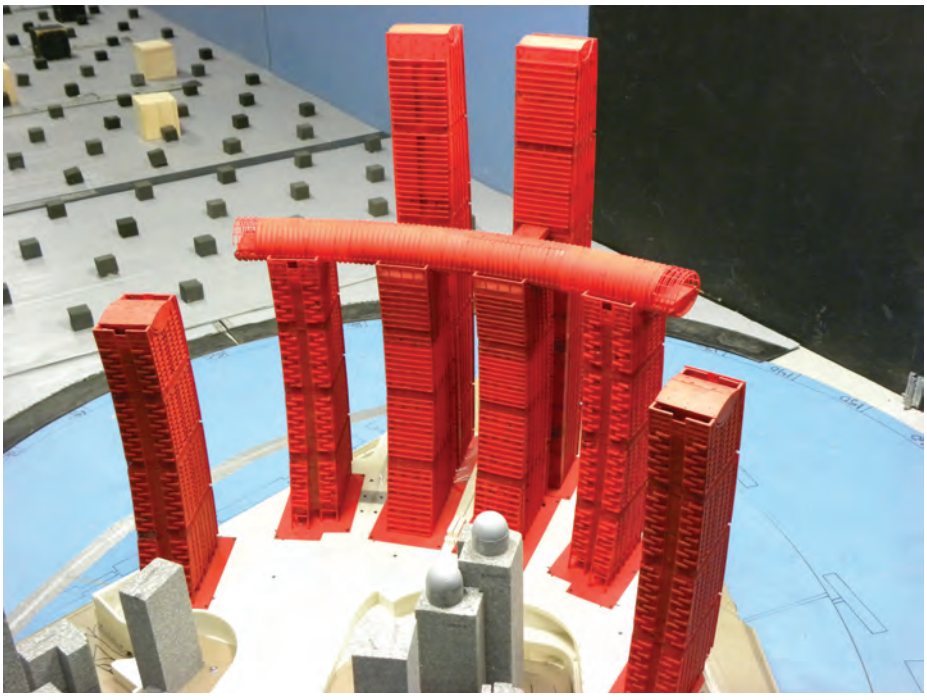

Figure 1. Wind tunnel photo for HFPI test (Source: CapitaLand and RWDI)
图1. 高平压力积分风洞试验照片（来源：凯德中国与RWDI）

等、测压试验会被一定程度上受到限制，从属面积的计算也需更加精细以确保正确。为此，本文在试验设计阶段，参考了大量的工程经验，对测压点的布置和数量进行了精细的设计。

对于连体结构的设计，有两点必须予以考虑：（a）整体结构的受力，包括子结构的连体性和结构模态，以及（b）子结构之间的相互作用力，包括由连体结构传递的力、以及由子结构产生在连体结构上的力（Xie，2005）。

重庆来福士广场项目是世界最大开发项目之一。项目位于中国重庆渝中区的朝天门广场和解放碑之间。整体建筑由八个塔组成，高度介于182米至310米之间。每个塔弯曲成船帆形状。塔2和塔5的空中花园贯穿其他塔。由图一所示，该建筑外形复杂，如有大量阳台。为保证可靠的结果，本文进行了高频测力试验（HFFB）和高频测压试验（HFPI）（图1）。由此得到用于结构设计的风荷载。MFB系统被用于进行连体塔结构的分析。

除天桥外，确定风荷载的困难还包含了多塔连体和复杂地貌。通过风场地貌研究，风洞试验内的项目场地风剖面包含了邻近丘陵山地地貌。

本文陈述了风剖面模拟方法及风场地貌测量分析结果。进一步，本文讨论了包括连体结构在内的风致结构响应。

试验设置

整体设置

如图2所示，本文所研究的结构由八个塔组成。结构俯视图可参见图3。其中六个塔由天桥相连。在塔3N 和3S，以及塔4N和4S间有人行天桥相连。但是由于这些天桥使用了伸缩缝连接，可以考虑为没有结构连接。塔2， 3S， 4S和5由天桥所连接，并且为结构连体（图2）。

对于MFB试验，根据建筑设计图纸，本文设计了一个缩尺比为1:400风洞试验测力模型。该模型在包含了460米范围内以建成建筑物的地貌环境下进行风洞试验（图4）。塔2，3S，3N，4S，4N和5 分别固定在测力天平上并同时测量。同样，本文也设计了一个1:400 的测压模型。其中塔2，3S，3N，4S，4N和5一共包含了1000各测压点。在试验中，所有测压点通过由1024各通道的扫描阀同步测量。

由于项目模型的大小，阻塞度成为一个需要考虑的问题，Maskell(1963)和Gould(1969)进行了钝体阻塞度修正的研究，他们发现大部分的阻塞效应能够通过以下方法修正。Irwin（1979)研究了边界

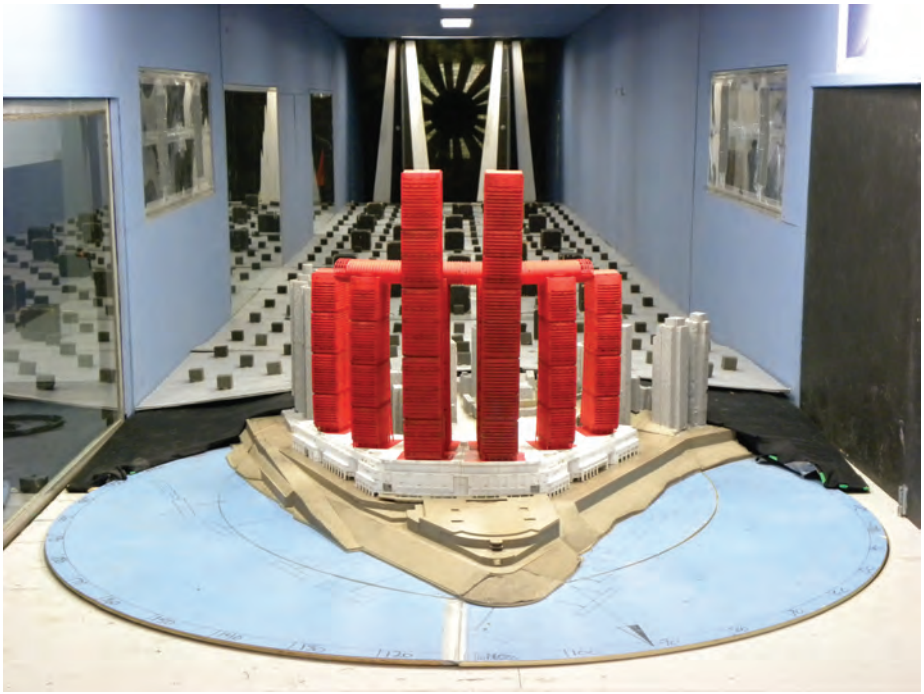

Figure 2. RCCQ development (Source: CapitaLand and RWDI)
图2. 重庆来福士广场项目（来源：凯德中国与RWDI）

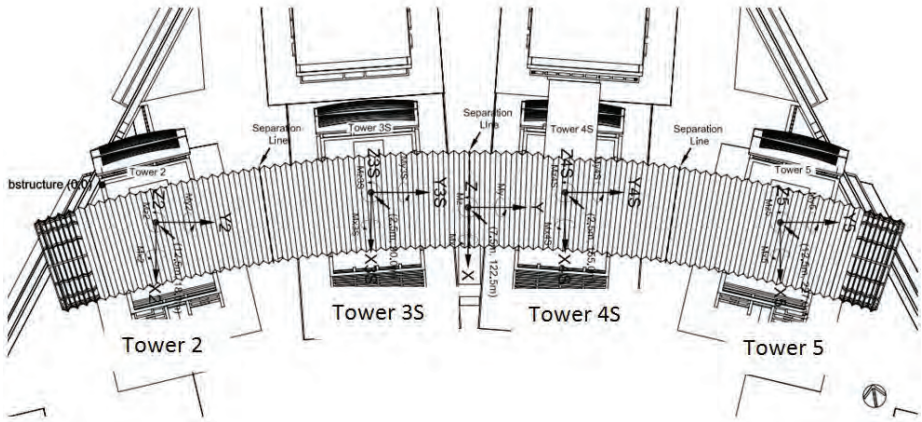

Figure 3. Coordinate systems for structural loading (Source: CapitaLand and RWDI)
图3. 结构荷载坐标系统（来源：凯德中国与RWDI）

and 4S. However, there are expansion joints on these bridges so that these towers are not considered as being structurally linked. A sky bridge conservatory sits on the tops of towers 2, 3S, 4S and 5, and is structurally connected to all four towers (Figure 2).

For the MFB test, a 1:400 scale force-balance model of the proposed development was constructed using the architectural drawings. The model was tested in the presence of all existing surroundings within a full-scale radius of 460m in a boundary layer wind tunnel (Figure 4). The models of towers 2, 3S, 3N, 4S, 4N and 5 were mounted on six force-balance flexures and tested simultaneously. Similarly, a 1:400 scale HFPI model of the whole development was constructed and the models of towers 2, 3S, 4S, and 5 were instrumented with 1,000 pressure taps. During the wind tunnel test, these pressure taps were measured simultaneously by using a Scanivalve system with 1,024 channels.

Due to the size of the model, we consider the blockage effect on the test results. Corrections for the blockage effect for bluff bodies were investigated by Maskell (1963) and Gould (1969) and they found that most blockage effects can be corrected for by assuming that the reference dynamic pressure. Irwin (1979) investigated the related problem of the effect of a ramp on the boundary layer profile. These approaches are applied in the wind tunnel test and analysis.

Topographical Measurements

In the lowest layer of the atmosphere, the wind is slowed down due to the drag effect of features on the Earth's surface such as vegetation, the ground roughness and human construction. Within this atmospheric boundary layer, the mean wind speed generally increases with height until the top of the layer is reached, at which point surface drag no longer plays a role. The mean speed implies an average speed over a

层风剖面下的斜坡效应的相关问题，这些方法被综合使用在我们的试验和分析中。

地貌测量Topographical Measurements

在大气边界层的最底部，风速由于地表，如植被，地面粗糙及人造结构，产生的阻力效应被降低。在此大气边界层中，平均风速由地表起逐渐提高，直到边界层的顶部，地表阻力效应不在产生影响。此处所说的平均风速为小时平均风。边界层高度为一个变化量，通常情况下为1000米或更高（见ESDU）。

重庆是著名的山城。为此对于项目场地处的风环境需要有特殊考虑。在项目场地处的山地谷道会对风速、紊流度、风向角产生多种效应。由于实地测量非常困难，这些效应最好通过地貌模型试验确定。本文通过一个1：3000 的地貌模型试验，研究了项目场地附近的风环境，并由于在1：400的模型试验中模拟了该风场环境（图5）。

通过改变地面粗糙度和调整紊流发生器，来流风向的各种地表粗糙度可以在模型尺度下进行重现。该技术的具体实现可参见Irwn（Irwn，1979）。

在强风中，在大气边界层内的平均风剖面可以用指数率来描述：

$$U_g = U_g \left(\frac{Z}{Z_g}\right)^{\alpha}$$

其中：U 是平均风速； Ug是梯度风速（在边界层顶部的风速）；Z是高出零平面（d）的高度；Zg是边界层高度，即梯度高度； α 是表面粗糙指数。竖向高度，Z ，是从零平面（d）处算起。零平面的计算可参考Simiu 和Scanlan（1978）。通常情况下，d 可以取20米。对于开阔地貌或者乡村地貌，d 的取值不是非常重要。

速度折减系数，F，计算按照国标50009–2012的要求，使两种尺度下的峰值压强保持一致。其计算可以表达为：

$$U_{ref} = F \cdot U_{500m\_open}$$

$$F = \left\{\frac{U_z\left[1+g\cdot I_u(z)\right]}{U_{500m\_open}}\right\}_{1:3000} \cdot \left\{\frac{U_{ref}}{U_z\cdot\left[1+g\cdot I_u(z)\right]}\right\}_{1:400}$$

其中z是高度，Uz是在z高度处的平均风速，Iu(z)是在z高度处的紊流度，U500m_open 是500米高度处开阔地貌下的平均风速，Uref是在1：400模型参考高度处（480米）的参考风速，g是峰值系数，其被定义为峰值和平均风速的差值与湍流均方根值的比值。

本文在参照高度处对平均风速剖面和峰值速度进行了不同角度的对比。

period of about one hour. The height of the boundary layer is variable but, in strong winds, can be 1,000 m or more (see ESDU).

Chongqing is well known as a hilly city which is also surrounded by hills and low mountains. Special consideration was required to provide appropriate modeling of the wind characteristics at the RCCQ project site. The mountains and valleys surrounding the site can produce various effects on the wind velocity, turbulence intensity and local wind direction at the site. In the absence of full scale measurements, which would be extremely difficult to obtain, these effects are best determined through topographical model studies. Using a 1:3,000 scale topographical model study, the wind characteristics at the study site were determined and then simulated for the subsequent 1:400 scale model (Figure 5).

By varying the floor roughness and turbulence generators, the effects of various types of terrain roughness upwind of the turntable can be reproduced at model scale. A detailed explanation of these techniques is provided by Irwin (1979).

In strong winds, the mean speed profile in the atmospheric boundary layer over most terrains is found to be well represented by the power law expression:

$$U_g = U_g \left(\frac{Z}{Z_g}\right)^{\alpha}$$

Where U is mean wind speed; Ug is gradient wind speed (value of U at the top of the boundary layer); Z is height above zero plane displacement height, i.e., d; Zg is depth of boundary layer, i.e., gradient height; and α is surface roughness index. Note that the vertical height, Z, is referenced from the zero plane displacement height, d. The value of d may be determined from Simiu and Scanlan (1978). A representative value of d for urban terrain is 20 m. For open and suburban terrains, d is insignificant.

The velocity scaling factor, F, is based on the concept of matching peak gust pressure between the two scale models at the matching heights at full scale, as required by the Building Code of China, GB50009-2012 which led to the following expression:

$$U_{ref} = F \cdot U_{500m\_open}$$

$$F = \left\{\frac{U_z\left[1+g\cdot I_u(z)\right]}{U_{500m\_open}}\right\}_{1:3000} \cdot \left\{\frac{U_{ref}}{U_z\cdot\left[1+g\cdot I_u(z)\right]}\right\}_{1:400}$$

Where z is the height of interest, Uz is the mean wind speed measured at the height of interest, Iu(z) is the turbulence intensity at the height of interest, U500m_open is the wind speed specified at 500 m above open terrain, Uref is the mean wind speed measured at the reference height (480 m) on the 1:400 scale model, and g is the peak factor, defined as the ratio of the peak velocity fluctuation to the rms velocity. The comparison of the mean speed profiles and peak gust speed profiles at both matching heights will be provided on a direction-by-direction basis in the study.

风气候

为了预测建筑表面不同回归期的全尺度风压，风洞试验数据和数值风气候模型一同使用。风气候模型的建立基于重庆气象台,WMO #57516， 与1987 到2010年间的风速测量数据。该气象台站距离项目地点大概12公里以西。

风气象模型通过折减得到在离地500米高度处100 回归周期的小时平均风速为45.8m/s。该值与国标50009–2012中规定的数值一致。

通常情况下，单个或多个距离项目站点较近的气象台的风速数据将被用于建立风气候模

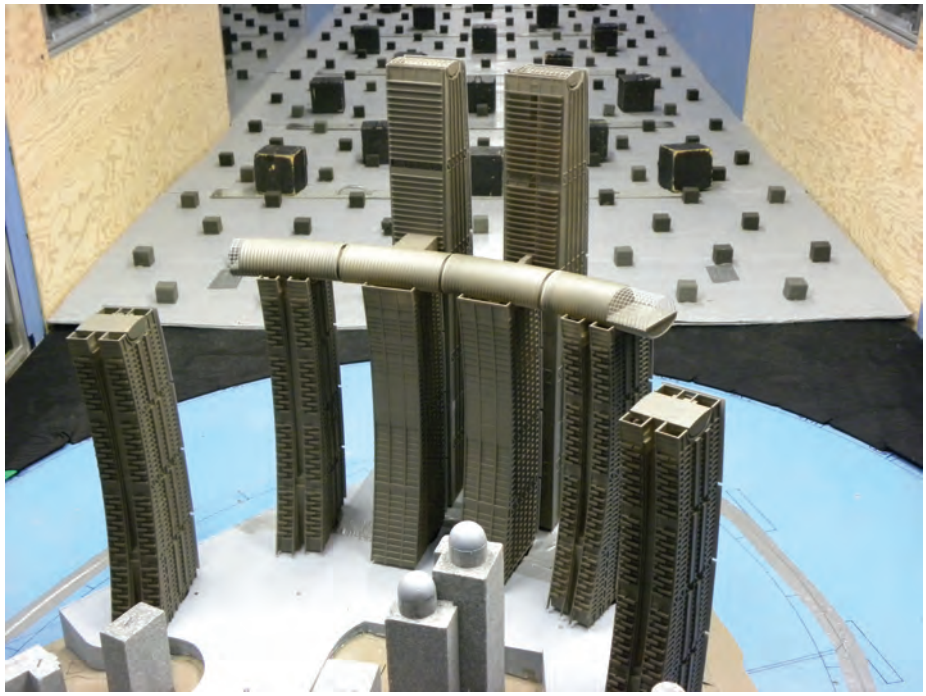

Figure 4. Wind tunnel photo for MFB test (Source: CapitaLand and RWDI)
图4. 多高频天平风洞试验照片（来源：凯德中国与RWDI）

Figure 5. Topographical wind tunnel photo (Source: CapitaLand and RWDI)
图5. 地貌试验风洞试验照片（来源：凯德中国与RWDI）

Wind Climate

In order to predict the full-scale wind pressures acting on the building as a function of return period, the wind tunnel data were combined with a statistical model of the local wind climate. The wind climate model was based on local surface wind measurements taken at Chongqing Meteorological Station, WMO #57516, between 1987 and 2010. The location of the Chongqing Meteorological Station is approximately 12 km west of the project site.

The wind climate model was scaled so that the magnitude of the wind velocity for the 100-year return period corresponded to a mean hourly wind speed of 45.8 m/s at a height of 500 m above ground in open terrain. This value is consistent with that identified in the Building Code of China, GB50009-2012.

Wind records taken from one or more locations near to the study site are generally used to derive the wind climate model. The data are analyzed to determine the probabilities of exceeding various hourly mean wind speeds from within each of 36 wind sectors at an upper level reference height above open terrain. This coincides with the height used to measure the reference dynamic pressure in the wind tunnel.

Results and Discussion

For the purpose of conducting an appropriate analysis, the development was divided into four substructures as described below:

1. Substructure 1 corresponds to Tower 2 and its tributary portion of the Conservatory (to midway between Towers 2 and 3S)
2. Substructure 2 corresponds to Tower 3S and its tributary portion of the Conservatory (from midway between Towers 2 and 3S to midway between Towers 3S and 4S)
3. Substructure 3 corresponds to Tower 4S and its tributary portion of the Conservatory (from midway between Towers 3S and 4S to midway between Towers 4S and 5)
4. Substructure 4 corresponds to Tower 5 and its tributary portion of the Conservatory (to midway between Towers 4S and 5)

The reference axis system used to define the forces and moments for the entire structure and individual substructures is illustrated in Figure 3.

After wind tunnel tests of both MFB and HFPI model systems, the test data were analyzed with the building structure properties. Fourteen mode shapes were included in the consideration. Test results for the important model shapes can be seen in Figure 6, which shows that wind induced responses on different model shapes caused significantly different tower interactions. The 1st and 2nd models are Y direction sway and X direction sway of the 4 towers simultaneously with the periods of 6 seconds and 4.53 seconds, respectively. The 3rd mode is the torsion of the entire structure with the period of 3.43 seconds. The higher modes become more complicated that the individual towers behave very different due to the complications of the structure system and linkage constraints. Therefore, wind induced structure responses of each structure at different mode shapes and frequencies can be excited by strong winds and the multi substructure dynamic analysis takes into account these impacts on the structures.

The overall wind-induced 100-year return period loads for each wind direction are presented in Figures 7a, 7b, 7c, and 7d for Towers 2, 3S, 4S, and 5, respectively. The loads in these figures are the values based on

型。这些数据用于确定在参考高度处每个风向角（一共36个风向角）内超越某一平均风速的概率。该高度处需和风洞试验中的参考动压测量高度一致。

结果及讨论

为了合理分析结果，整体结构被分割为了四个子结构：

1. 子结构1代表塔2以及空中花园所对应的从属面积（塔2和3S之间）。
2. 子结构2代表塔3S以及空中花园所对应的从属面积（从塔2和3S之间到塔3S和4S之间）。
3. 子结构3代表塔4S以及空中花园所对应的从属面积（从塔3S和4S之间到塔4S和5之间）。
4. 子结构4代表塔5以及空中花园所对应的从属面积（塔4S和5之间）。

图3给出了用于定义力和力矩的参考轴。

结构物理参数用于分析由MFB和HFPI试验测的数据。十四个模态用于本文的分析。图6中给出了关键模态的测试结果。可见，在不同模态下，风致响应是不同的。第一、二阶模态四个塔在X和Y方向的同时

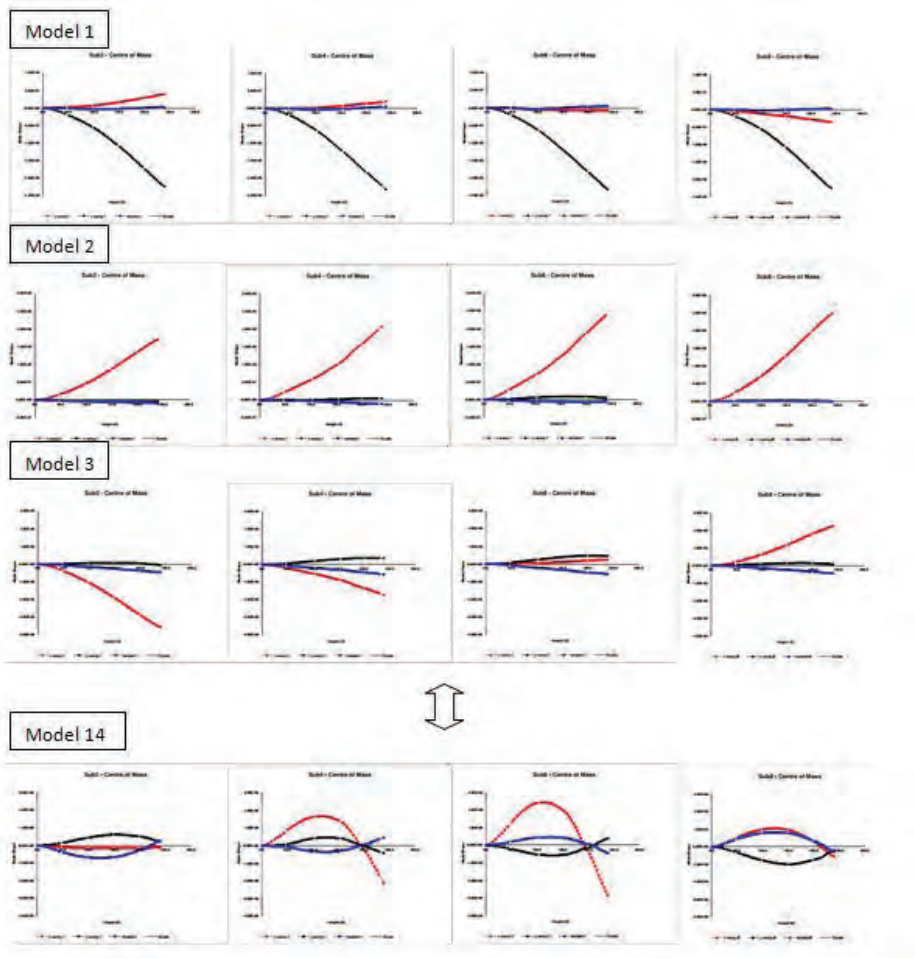

Figure 6. Selected mode shapes (Source: CapitaLand and RWDI)
图6. 振型曲线样例（来源：凯德中国与RWDI）

the design wind speed, assuming this wind speed applies equally in all directions. The square symbols are the mean wind loads, the diamond symbols are the maximum loads, and the triangle symbols are minimum loads. This information simply illustrates the raw source data used in predicting the peak design loads. These figures present the result comparisons of the MFB and HFPI test systems. Between the tests of MFB and HFPI, there were some minor design changes, such as a small bridge added between towers T3S and T3N and some structure property revision. Due to these minor differences in geometry, the results show some discrepancies. However, the overall comparisons are close and within experimental error allowances.

From the wind responses in Figure 7, it can be seen that the maximum and minimum loads of each substructure do not happen at the same wind direction. Based on the time history of the simultaneous wind tunnel measurement, the peak loads of the individual substructure do not happen at the same time too. Therefore, individual tower measurements and analysis may provide peak loads for each tower, but summation of the peak loads of individual towers may lead to conservative results and may cause structure over design. In order to achieve optimum design, based on these results, multi structure analyses were conducted. Figure 8 illustrates some of the loading combinations for the structural design that considered different responses from individual towers. The loads were determined using the first 14 building vibration frequencies. The loads have been provided for a total damping ratio of 2%.

In using the predicted effective static wind loads, it is important to consider how the x, y, and z components of the wind load should be combined when applying them to each substructure. For the structural design of each individual substructure, as well as the entire structure, the set of recommended load combination factors provided in Table 1 were considered with the simultaneous application of the wind loads provided as the results of the analyses. These are the load combinations that will produce the peak overall wind-induced loads for each substructure as well as for the entire structure. There are 122 load combinations obtained and provided, which represent each of eight possible sign sets (+++, ++-, +-+, etc.) with each component – Fx, Fy, and Mz – for one or more diaphragm, or the entire structure, reaching its individual maximum percentages for that sign set.

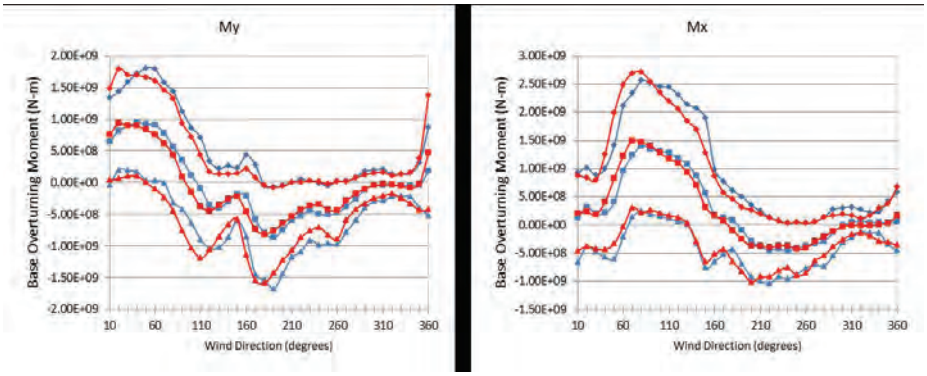

Figure 7a. Raw overall base moments of Tower 2 at "Base" – 100 year return period wind speed (Source: CapitaLand and RWDI)
图7a. 塔2的基底弯矩风荷载——100年重现期风速（来源：凯德中国与RWDI）

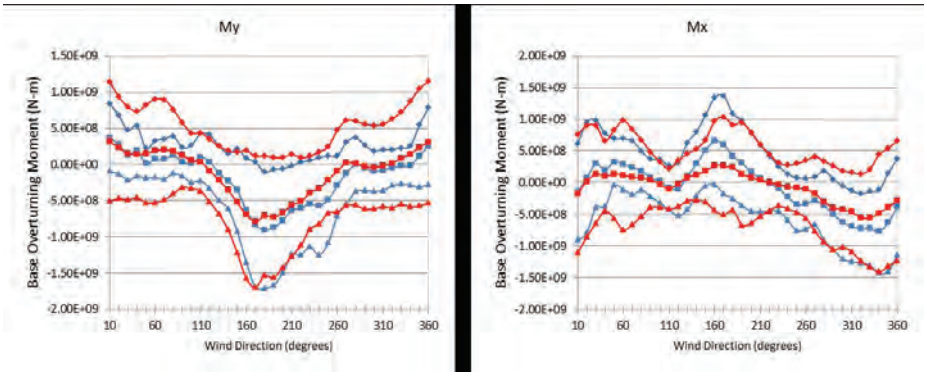

Figure 7b. Raw overall base moments of Tower 3S at "Base" – 100 year return period wind speed (Source: CapitaLand and RWDI)
图7b. 塔3S的基底弯矩风荷载——100年重现期风速（来源：凯德中国与RWDI）

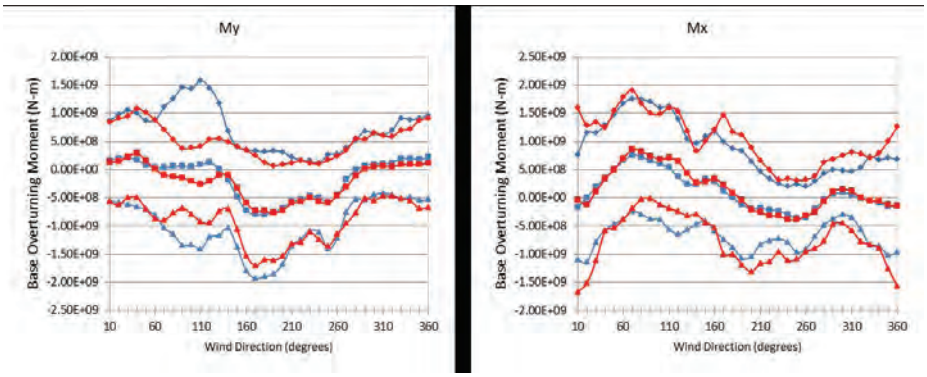

Figure 7c. Raw overall base moments of Tower 4S at "Base" – 100 year return period wind speed (Source: CapitaLand and RWDI)
图7c. 塔4S的基底弯矩风荷载——100年重现期风速（来源：凯德中国与RWDI）

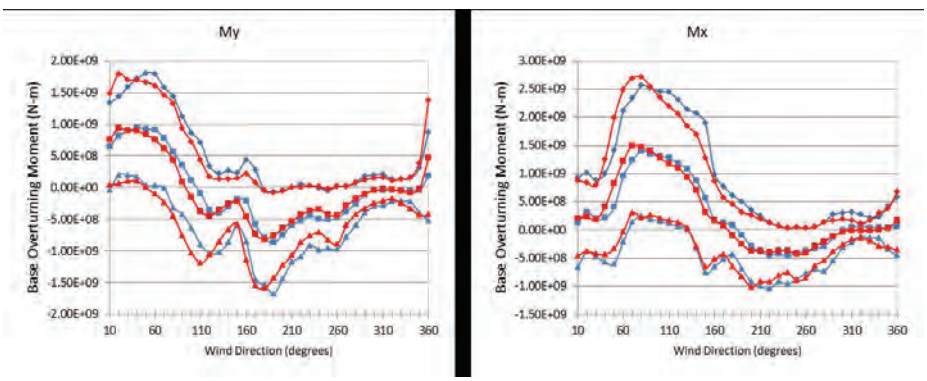

Figure 7d. Raw overall base moments of Tower 5 at "Base" – 100 year return period wind speed (Source: CapitaLand and RWDI)
图7d. 塔5的基底弯矩风荷载——100年重现期风速（来源：凯德中国与RWDI）

Load Combination	Tower 2 Loads from Table 3b-1 x Load Combination Factor			Tower 3S Loads from Table 3c-1 x Load Combination Factor			Tower 4S Loads from Table 3e-1 x Load Combination Factor			Tower 5 Loads from Table 3g-1 x Load Combination Factor		
1a	+100% x Fx2	+35% x Fy2	+40% x Mz2	+50% x Fx3S	+20% x Fy3S	+20% x Mz3S	+35% x Fx4S	+20% x Fy4S	+20% x Mz4S	+55% x Fx5	+20% x Fy5	+20% x Mz5
2a	+100% x Fx2	+35% x Fy2	-55% x Mz2	+50% x Fx3S	+20% x Fy3S	-45% x Mz3S	+35% x Fx4S	+20% x Fy4S	-40% x Mz4S	+55% x Fx5	+20% x Fy5	-30% x Mz5
3a	+100% x Fx2	-30% x Fy2	+40% x Mz2	+50% x Fx3S	-10% x Fy3S	+10% x Mz3S	+35% x Fx4S	-10% x Fy4S	+10% x Mz4S	+55% x Fx5	-20% x Fy5	+10% x Mz5
4a	+100% x Fx2	-30% x Fy2	-55% x Mz2	+50% x Fx3S	-10% x Fy3S	-45% x Mz3S	+35% x Fx4S	-10% x Fy4S	-40% x Mz4S	+55% x Fx5	-20% x Fy5	-30% x Mz5
5a	-75% x Fx2	+30% x Fy2	+30% x Mz2	-80% x Fx3S	+10% x Fy3S	+20% x Mz3S	-75% x Fx4S	+10% x Fy4S	+30% x Mz4S	-45% x Fx5	+10% x Fy5	+20% x Mz5
6a	-75% x Fx2	+30% x Fy2	-35% x Mz2	-80% x Fx3S	+10% x Fy3S	-20% x Mz3S	-75% x Fx4S	+10% x Fy4S	-20% x Mz4S	-45% x Fx5	+10% x Fy5	-20% x Mz5
7a	-75% x Fx2	-50% x Fy2	+30% x Mz2	-80% x Fx3S	-15% x Fy3S	+20% x Mz3S	-75% x Fx4S	-15% x Fy4S	+30% x Mz4S	-45% x Fx5	-10% x Fy5	+20% x Mz5
8a	-75% x Fx2	-50% x Fy2	-35% x Mz2	-80% x Fx3S	-15% x Fy3S	-10% x Mz3S	-75% x Fx4S	-15% x Fy4S	-10% x Mz4S	-45% x Fx5	-10% x Fy5	-10% x Mz5
9a	+55% x Fx2	+100% x Fy2	+30% x Mz2	+30% x Fx3S	+60% x Fy3S	+20% x Mz3S	+30% x Fx4S	+20% x Fy4S	+45% x Mz4S	+20% x Fx5	+20% x Fy5	+25% x Mz5
10a	+55% x Fx2	+100% x Fy2	-45% x Mz2	+30% x Fx3S	+60% x Fy3S	-50% x Mz3S	+30% x Fx4S	+20% x Fy4S	-20% x Mz4S	+20% x Fx5	+20% x Fy5	-20% x Mz5

Figure 8. Load combination factors for simultaneous application of effective static wind loads. (Source: CapitaLand and RWDI)
图8. 等效静风荷载的整体荷载组合系数（来源：凯德中国与RWDI）

Load Combination	Conservatory 2 Loads from Table 3i-1 x Load Combination Factor				Conservatory 3S Loads from Table 3j-1 x Load Combination Factor				Conservatory 4S Loads from Table 3k-1 x Load Combination Factor				Conservatory 5 Loads from Table 3l-1 x Load Combination Factor			
27	+20% x Fx2	-60% x Fy2	+20% x Mz2	+25% x Fz2	-20% x Fx3S	+30% x Fy3S	-25% x Mz3S	+50% x Fz3S	-20% x Fx4S	+30% x Fy4S	-20% x Mz4S	+50% x Fz4S	-20% x Fx5	+30% x Fy5	-20% x Mz5	+25% x Fz2
28	+20% x Fx2	-60% x Fy2	-30% x Mz2	+25% x Fz2	-20% x Fx3S	+30% x Fy3S	+30% x Mz3S	+50% x Fz3S	-20% x Fx4S	+30% x Fy4S	+30% x Mz4S	+50% x Fz4S	-20% x Fx5	+30% x Fy5	+30% x Mz5	+25% x Fz2
29	-20% x Fx2	+80% x Fy2	-30% x Mz2	+25% x Fz2	+20% x Fx3S	-25% x Fy3S	+20% x Mz3S	+50% x Fz3S	+20% x Fx4S	-35% x Fy4S	+40% x Mz4S	+50% x Fz4S	+20% x Fx5	-35% x Fy5	+20% x Mz5	+25% x Fz2
30	-20% x Fx2	+80% x Fy2	+20% x Mz2	+25% x Fz2	+20% x Fx3S	-25% x Fy3S	-40% x Mz3S	+50% x Fz3S	+20% x Fx4S	-35% x Fy4S	-30% x Mz4S	+50% x Fz4S	+20% x Fx5	-35% x Fy5	-20% x Mz5	+25% x Fz2
31	+80% x Fx2	-20% x Fy2	-20% x Mz2	+25% x Fz2	-35% x Fx3S	+20% x Fy3S	+20% x Mz3S	+50% x Fz3S	-45% x Fx4S	+20% x Fy4S	+20% x Mz4S	+50% x Fz4S	-20% x Fx5	+20% x Fy5	+20% x Mz5	+25% x Fz2
32	+80% x Fx2	+20% x Fy2	-20% x Mz2	+25% x Fz2	-35% x Fx3S	-20% x Fy3S	+20% x Mz3S	+50% x Fz3S	-45% x Fx4S	-20% x Fy4S	+20% x Mz4S	+50% x Fz4S	-20% x Fx5	-20% x Fy5	+20% x Mz5	+25% x Fz2
33	-45% x Fx2	-20% x Fy2	-20% x Mz2	+25% x Fz2	+60% x Fx3S	+20% x Fy3S	+20% x Mz3S	+50% x Fz3S	+40% x Fx4S	+20% x Fy4S	+20% x Mz4S	+50% x Fz4S	+40% x Fx5	+20% x Fy5	+20% x Mz5	+25% x Fz2
34	-45% x Fx2	+20% x Fy2	-20% x Mz2	+25% x Fz2	+60% x Fx3S	-20% x Fy3S	+20% x Mz3S	+50% x Fz3S	+40% x Fx4S	-20% x Fy4S	+20% x Mz4S	+50% x Fz4S	+40% x Fx5	-20% x Fy5	+20% x Mz5	+25% x Fz2

Figure 9. Differential load combination factors for simultaneous application of effective static wind loads. (Source: CapitaLand and RWDI)
图9. 等效静风荷载的差异荷载组合系数（来源：凯德中国与RWDI）

For example, Load Combination 1a in Figure 8 requires the simultaneous application of the following:

- +100% of the Fx2 loads, +35% of the Fy2, and +40% of the Mz2 for Tower 2.
- +50% of the Fx3S loads, +20% of the Fy3S, and +20% of the Mz3S for Tower 3S;
- +35% of the Fx4S loads, +20% of the Fy4S, and +20% of the Mz4S for Tower 4S; and,
- +55% of the Fx5 loads, +20% of the Fy5, and +20% of the Mz5 for Tower 5.

The tests of all four towers are conducted simultaneously so that the dynamic responses can be considered to be happening at the same time. Interestingly, one can see that the maximum wind-induced structural loads for the entire structure do not occur at the time that all towers are experiencing maximum loads.

The multi-substructure analysis shows the load combinations that provide optimized loads for the design of the entire structure and save the extra construction cost from an unnecessarily conservative approach.

In order to design for the loads of the towers acting on the conservatory linkage (e.g., compression, tension and shear), differential load cases also need to be considered. As an example, Figure 9 provides the maximum differential loading scenarios (i.e., tension, compression, shear) on the link between Tower 2 and Tower 3S. The differential loading scenarios of Tower 3S and Tower 4S, and Tower 4S and Tower 5 were also subjected to the same analysis but are not included as part of this paper.

摆动。其周期分别为6秒和4.53秒。第三阶模态是整体结构在周期为3.43秒下的扭转。由于整体结构的复杂性和连体性，结构在更高阶的模态下的振动形态更为复杂，各塔的振动形态表现极为不同。因此，可以看出在强风下，各子结构在不同模态下的振动可由强风激起。通过多子结构动态分析，这些对结构的作用可以得到考虑。

图7a、7b、7c和7d分别给出了对塔2、3s、4s和5 在不同风向的100回归期的风荷载。这些风荷载是基于设计风速得出，并假设可应用于任何风向角。图中，方形代表平均风荷载，菱形代表最大风荷载，三角形代表最小风荷载。这些信息示意了用于计算峰值设计荷载的原始数据。这些图也给出了MFB和HFPI试验的比较。在MFB和HFPI试验期前，设计略有更改，比如在塔T3S和T3N之间增加了一座小型天桥，另外一些结构参数略有变动。由于这些几何差异，结果会有所差异。但是，俩组试验的整体比较非常接近，差别可以认为在误差范围内。

Conclusions

1. Structural links may have significant effects on wind-induced dynamic response. Only proper wind tunnel tests and multi-substructure dynamic analyses can provide a sufficient number of wind load cases to meet structural design needs.
2. Multi-substructure dynamic analysis based on simultaneous testing of MFB or HFPI model systems can provide optimized wind loading so that more economical designs can be achieved.
3. MFB and HFPI model systems both can provide good results and the comparison of test results shows good agreement between the models.
4. The Multi-force-balance system (MFB) is a practical method for studying structurally linked tower structures and provides accurate results for the structure design.

在图7中所显示的风致响应，可以看出不同子结构的最大、最小荷载没有发生在用一个风向角上。通过对风洞测试时程观察，这些峰值荷载也不是同时发生的。因此，单塔测量虽然可以提供每个塔的峰值荷载，但简单将峰值荷载相加可能造成过度保守的结构设计。为了达到优化设计，本文进行了多结构分析。图8给出了一些不同单塔响应下的荷载组合。本文使用了前十四阶自振频率。结构整体阻尼假设为2%。

在使用等效静荷载时，必须考虑如何对荷载在x，y，and z 方向的分量进行组合并应用到子结构上。对于结构设计，表一中给出了建议的荷载组合。这些荷载组合能够产生子结构和整体结构的峰值响应。一共有122种荷载组合，分表代表不同的符合组合（+++，++−，+−+等）和不同的荷载分量（Fx，Fy和Mz）图，或者整体结构达到该分量下的最大值。

比如，在图8中的荷载组合1a需要同时考虑：

- 对于塔2，+100% 的 Fx2，+35% 的 Fy2，以及 +40% 的 Mz2 。
- 对于塔3S,+50% 的 Fx3S，+20% 的 Fy3S，以及 +20% 的 Mz3S。
- 对于塔4S，+35% 的 Fx4S ，+20% 的 Fy4S，以及 +20% 的 Mz4S。
- 对于塔5，+55% 的 Fx5，+20% 的 Fy5，以及 +20% 的 Mz5 。

所有四个塔同时测量，这样可以保证动力响应可以同时发生。有趣的是，最大的结构荷载没有发生在所有塔经历最大风荷载的时候。子结构分析显示荷载组合提供了优化的设计荷载并降低了由过度保守的荷载造成的额外建造成本。

对于天桥上的设计风荷载，本文对不同的荷载组合进行了考虑。比如，图9提供了塔2和塔3S连接处之间的最大力差值（即拉力，压力和剪力）。对于塔 3S 和 塔4S，以及 塔4S和塔5的连接处，本文也进行了相同的分析，但限于篇幅，此处不予表述。

结论

1. 结构连接可能对风致动力响应造成重要影响。只有通过风洞试验和多子结构动力分析才能够对设计需要提供足够的设计风荷载。
2. 基于MFB和HFPI试验的多子结构动力分析可以提供优化的设计荷载。
3. MFB和HFPI可以提供较为一致的试验结果。
4. 多天平测力系统可以应用于建构连体塔群的测试，并为结构设计提供准确的结果。

References:

Dragoiescu C., Garber J. and Suresh. K.K. (2006). **"A Comparison of Force Balance and Pressure Integration Techniques for Predicting Wind-Induced Responses of Tall Buildings"**, ASCE Structures Congress 2006 – Extreme Event Loading - Extreme Wind Engineering.

ESDU International. **"Wind Engineering Subseries Volumes 1A and 1A",** 1993 Edition, London, England.

Gould, R.W.F. (1969). **Wake Blockage Corrections in a Closed Wind Tunnel for One or Two Wall-Mounted Models Subject to Separated Flow.** UK Aeronautical Research Council Reports and Memoranda No. 3649, February, 1969.

Irwin, H.P.A.H. (1979). **Design and Use of Spires for Natural Wind Simulation.** National Research Council of Canada, NAE Report LTR-LA-233, August 1979.

Irwin, P.A. and Kochanski, W.W. (1995). **"Measurement of Structural Wind Loads Using the High Frequency Pressure Integration Method"**, Proc. ASCE Structures Congress, Boston, pp.1631-1634

Maskell, E.C. (1963). **Theory of Blockage Effects on Bluff Bodies and Stalled Wings in a Closed Wind Tunnel.** UK Aeronautical Research Council Reports and Memoranda No. 3400, November, 1963.

Reinhold, T.A. (1977). **Measurement of Simultaneous Fluctuating Loads of Multiple Levels of a Model of a Tall Building in a Simulated Urban Boundary Layer.** Ph.D., Blacksburg, Virginia, U.S.: Virginia Polytechnic Institute and State University.

Simiu, E. and Scanlan, R.H. **"Wind Effects on Structures",** John Wiley and Sons, NY, 1978.

Xie, J. and Irwin, P.A. (1998). **Application of the Force Balance Technique to a Building Complex.** Journal of Wind Engineering and Industrial Aerodynamics, Vol 77&78(1998) :579-590.

Xie, J. and To, A. (2005). **Design-Orientated Wind Engineering Studies for CCTV New Building,** In Proceedings of the 6th Asia-Pacific Conference on Wind Engineering, Seoul, Korea, 2005

Xie, J. and Irwin, P.A. (2001). **Wind-Induced Response of a Twin-Tower Structure.** Wind & Structures, an International Journal, Vol. 4, No.6.